Title
Protein Cross-Linking and Oligomerization through Dityrosine Formation upon Exposure to Ozone

Journal
Environmental Science and Technology, 49(18)

ISSN
0013-936X

Authors
Kampf, Christopher J
Liu, Fobang
Reinmuth-Selzle, Kathrin
et al.

Publication Date
2015-09-15

DOI
10.1021/acs.est.5b02902

Peer reviewed

Environmental Science & Technology

Article

pubs.acs.org/est

Protein Cross-Linking and Oligomerization through Dityrosine Formation upon Exposure to Ozone

Christopher J. Kampf,[*,†,‡,§] Fobang Liu,[‡,§] Kathrin Reinmuth-Selzle,[‡] Thomas Berkemeier,[‡] Hannah Meusel,[‡] Manabu Shiraiwa,[‡] and Ulrich Pöschl[‡]

[†]Institute of Inorganic and Analytical Chemistry, Johannes Gutenberg University Mainz, 55128 Mainz, Germany

[‡]Multiphase Chemistry Department, Max Planck Institute for Chemistry, 55128 Mainz, Germany

Supporting Information

ABSTRACT: Air pollution is a potential driver for the increasing prevalence of allergic disease, and post-translational modification by air pollutants can enhance the allergenic potential of proteins. Here, the kinetics and mechanism of protein oligomerization upon ozone (O_3) exposure were studied in coated-wall flow tube experiments at environmentally relevant O_3 concentrations, relative humidities and protein phase states (amorphous solid, semisolid, and liquid). We observed the formation of protein dimers, trimers, and higher oligomers, and attribute the cross-linking to the formation of covalent intermolecular dityrosine species. The oligomerization proceeds fast on the surface of protein films. In the bulk material, reaction rates are limited by diffusion depending on phase state and humidity. From the experimental data, we derive a chemical mechanism and rate equations for a kinetic multilayer model of surface and bulk reaction enabling the prediction of oligomer formation. Increasing levels of tropospheric O_3 in the Anthropocene may promote the formation of protein oligomers with enhanced allergenicity and may thus contribute to the increasing prevalence of allergies.

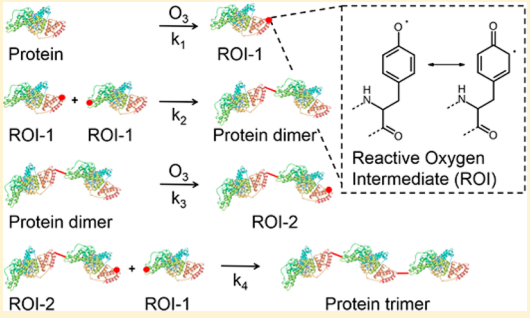

1. INTRODUCTION

The prevalence of allergies is increasing worldwide,[1,2] and air pollution has been identified as one of the factors potentially responsible for this trend, but the underlying chemical mechanisms remain unclear.[3] Air pollutants can directly affect the immune system, e.g., by inducing inflammation or oxidative stress,[4−7] and reactive trace gases like ozone (O_3) and nitrogen dioxide (NO_2) can induce post-translational modifications altering the immunogenicity of proteins.[8−12]

Atmospheric aerosols carry a variety of allergenic proteins in plant pollen, fungal spores, animal secretions and excrements. Besides these mostly larger particles (coarse mode particles, >1−2 μm diameter), several processes might also lead to the occurrence of allergenic proteins in fine mode particles (<1 μm), which may enter deeper into the respiratory tract. Such processes include the release of cytoplasmic granules from pollen (PCGs),[13] fragmentation of airborne cellular material,[14] and transfer of allergenic proteins onto fine mode particles (e.g., refs 14 and 15). Therefore, airborne allergenic proteins can be directly exposed to air pollution, such as O_3 and NO_2, promoting post-translational modifications like tyrosine (Tyr, Y) nitration.[16] Although a number of studies already investigated general mechanisms and kinetics of protein O_3 uptake and nitration,[17−19] analysis of site selectivity of protein nitration by O_3 and NO_2,[20] or specifically studied specific relevant aeroallergens, e.g., the major birch pollen allergen Bet v 1,[8,21,22] much less is known about oligomerization processes for proteins at atmospherically relevant concentrations of O_3.

The (transient) formation of homodimers or oligomers has been reported for a number of allergenic proteins.[23−29] Such dimers, typically formed by colocalization at high protein concentrations encountered in living cells, were observed in 80% of 55 allergen crystal structures and should show an enhanced allergenicity due to facilitated cross-linking of IgE antibodies at FceRI receptors on effector cells.[30] For Bet v 1.0101, it has recently been shown that the wild-type allergen partly contains a Y5C mutation and that a disulfide-bridge mediated stabilization of a dimeric form, which preferentially induced a T_H2 immune response.[28]

In this study, we investigate the formation of oligomers of proteins upon their exposure to atmospherically relevant concentrations of O_3. Bovine serum albumin (BSA) was used as a model protein, because O_3 uptake kinetics and rate constants are available in the literature.[17] Coated-wall flow tube and liquid phase experiments were performed to study the mechanism and kinetics of protein oligomerization under varying environmental conditions using size exclusion chromatography, fluorescence spectroscopy, gel electrophoresis, and a kinetic modeling approach.

Received: February 11, 2015
Revised: August 18, 2015
Accepted: August 19, 2015
Published: August 19, 2015

DOI: 10.1021/acs.est.5b02902
Environ. Sci. Technol. 2015, 49, 10859−10866

2. EXPERIMENTAL SECTION

2.1. Materials. Bovine serum albumin (BSA, A5611-1G), ammonium acetate (>98%, 32301-500G), trifluoroethanol (TFE, T63002), ammonium bicarbonate (A6141-25G), dithiothreitol (DTT, D5545-5G), and iodoacetamide (IAM, I6125-5G) were purchased from Sigma-Aldrich (Germany). 10× Tris/glycine/SDS (161-0732), 2× Lammli sample buffer (161-0737) were from Bio-Rad Laboratories (USA). PD-10 desalting columns were obtained from GE Healthcare (Germany). Sodium hydroxide (NaOH) was purchased from Merck (Germany). High purity water (18.2 MΩ m) for chromatography was taken from an ELGA LabWater system (PURELAB Ultra, ELGA LabWater Global Operations, UK). For other purposes, high purity water (18.2 MΩ m) was autoclaved before used if not specified otherwise.

2.2. Protein O_3 Exposure Setup. BSA solutions (0.6 mL; 3.33, 0.33, 0.07, and 0.03 mg mL^{-1} concentrations were used to achieve 2, 0.2, 0.04, and 0.02 mg of BSA coating for experiments discussed in section 3.2; for all other reactions, 0.33 mg mL^{-1} BSA solutions were used) were loaded into the glass tube and dried by passing a N_2 (99.999%) flow of ∼2.3 L min^{-1} through the rotated tube before the exposure experiment. The BSA-coated glass tube was then connected to the experimental setup. Figure S1 of the Supporting Information shows a schematic of the experimental setup. Ozone was produced from synthetic air passed through a mercury vapor lamp (Jelight Company, Inc., Irvine, USA) at 1.9 L min^{-1}. The O_3 concentration was controlled by varying the intensity of UV irradiation with an adjustable cover on the mercury vapor lamp. To control the relative humidity (RH), the gas flow was split; one flow was passed through a Nafion gas humidifier (MH-110-12F-4, PermaPure, Toms River, NJ, USA) operated with autoclaved high purity water, while the other flow remained dry. RH could be varied in a wide range by adjusting the ratio between the dry and humidified air flow. During the experiments, the standard deviation from the set RH values was <2% RH. The resulting air flow was then passed through the BSA-coated glass tube. O_3 concentration and RH were measured by commercial monitoring instruments (Ozone analyzer, 49i, Thermo Scientific, Germany; RH sensor FHA 646-E1C with an ALMEMO 2590-3 instrument, Ahlborn, Mess- und Regelungstechnik GmbH, Holzkirchen). After the respective exposure, the proteins were extracted from the glass tube with 1.5 mL of 1× Tris/glycine/SDS buffer to avoid precipitation of protein oligomers in the extract solution.

Additionally, to investigate further the role of protein phase state for the oligomerization process, the homogeneous reaction of dissolved protein and reactants were studied using a setup described in our previous study.[22] Briefly, O_3/synthetic air gas mixtures were bubbled directly through 1.5 mL 0.15 mg mL^{-1} BSA aqueous solutions (pH 7.1 ± 0.1; pH meter model WTW multi 350i; WTW, Weilheim, Germany) at a flow rate of 60 mL min^{-1}.

2.3. SEC-HPLC-DAD Analysis. Product analysis was performed using high-performance liquid chromatography coupled to diode array detection (HPLC-DAD, Agilent Technologies 1200 series). The HPLC-DAD system consisted of a binary pump (G1379B), an autosampler with thermostat (G1330B), a column thermostat (G1316B), and a photodiode array detector (DAD, G1315C). ChemStation software (Rev. B.03.01, Agilent) was used for system control and data analysis. Molecular weight (MW) separation by size exclusion chromatography (SEC) was carried out using a Bio SEC-3 HPLC column (Agilent, 300 Å, 150 × 4.6 mm, 3 μm) at a temperature of 30 °C. The mobile phase was 50 mM ammonium acetate (pH 6.8). The flow rate was 0.35 mL min^{-1} and the sample injection volume was 40 μL. The absorbance was monitored with the DAD at wavelengths of 220 and 280 nm.

A protein standard mix 15−600 kDa (69385, Sigma-Aldrich, Steinheim, Germany) containing thyroglobulin bovine (MW = 670 kDa), γ-globulins from bovine blood (MW = 150 kDa), albumin chicken egg grade VI (MW = 44.3 kDa), and Ribonuclease A (MW = 13.7 kDa) was used for the SEC column calibration (elution time vs log MW). For details, see the Supporting Information. It should be noted that SEC separates molecules according to their hydrodynamic sizes, thus only approximate molecular masses can be obtained by this calibration method. We report the formation of BSA oligomers as the temporal evolution in the ratios of the respective oligomers (dimer, trimer, and higher oligomers with $n \geq 4$) to the sum of monomer and all oligomer peak areas. The commercially available BSA contained also dimer and trimer variants of the protein. Therefore, the reported values were corrected for this background.

2.4. SDS-PAGE Analysis. Sodium dodecyl sulfate polyacrylamide gel electrophoresis (SDS-PAGE) was performed using Mini-PROTEAN TGX Any kD Stain-Free precast gels (Bio-Rad) according to the manufacturer's instructions. Briefly, samples were mixed with Lammli sample buffer and heated at 95 °C for 5 min prior to SDS-PAGE separation. A molecular weight marker (Precision Plus Protein Unstained Standards, 161-0363, Bio-Rad) was used for the calibration of the molecular weight scale. After the SDS-PAGE run, the gels were visualized on a ChemiDoc MP Imaging system with Image Lab software (Version 5.1, Bio-Rad). Molecular weights were determined using the MW Analysis Tool of the Image Lab software.

2.5. Fluorescence Spectroscopy. Fluorescence spectra were recorded on a LS 45 luminescence spectrometer (PerkinElmer, Inc., Waltham, MA, USA). A detailed instrument description is given in Pöhlker et al.[31] Samples were analyzed in a 10 × 10 × 40 mm UV quartz cuvette (Hellma Analytics, Müllheim, Germany). The photomultiplier tube detector voltage was 600 V. Excitation wavelengths were 240−400 nm (10 nm increments), whereas emission was recorded from 280 to 560 nm (0.5 nm increments). Excitation and emission slit widths were both set to 10 nm and a scan speed of 1500 nm min^{-1} was used.

3. RESULTS AND DISCUSSION

3.1. Protein Ozone Exposure Results in the Formation of Dityrosine Cross-Links. In a previous study, it has been demonstrated that O_3 can induce protein cross-linking in solution via the formation of dityrosine species. In this study, we explore this process and its kinetics for the heterogeneous and homogeneous reactions of proteins with O_3 at atmospherically relevant conditions.

For one set of homogeneous bulk solution experiments, the BSA samples were pretreated with DTT and IAM, according to the method described in Zhang, Yang, and Poschl[20] to exclude oligomer formation due to disulfide bridging. The alkylated BSA samples were then desalted with PD-10 columns according to the manufacturer's instructions and the eluates were used for the exposure experiments. Exemplary results are

DOI: 10.1021/acs.est.5b02902
Environ. Sci. Technol. 2015, 49, 10859−10866

illustrated in Figure 1. The BSA dimer (MW 141.9 kDa) and trimer (MW 195.8 kDa) bands clearly increased in intensity,

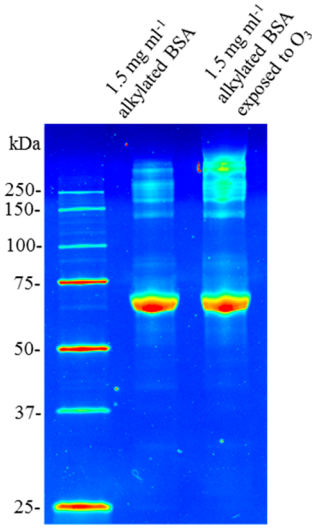

Figure 1. SDS-PAGE analysis of the homogeneous oligomerization of alkylated BSA exposed to 200 ppb O_3 for 2 h (false color illustration).

whereas the intensity of the monomer band (MW 65.1 kDa) is reduced. Interestingly, further bands at MWs higher than 250 kDa were found as well, indicating further oligomerization or agglomeration of BSA. Clearly, an O_3 induced formation of oligomers occurred and, more importantly, the cross-linking could not be attributed to the formation of intermolecular disulfide bonds because the thiol groups of the protein had been protected by alkylation before the exposure experiment. Additionally, the formation of dityrosine species in the reacted samples was confirmed by fluorescence spectrometry. Excitation and emission wavelengths of dityrosine in alkaline solution were taken from the literature (320 and 400 nm, respectively).[32] Accordingly, the pH of our samples was adjusted to 9.7 with 0.1 M NaOH before measurement. Figure 2a–c shows the excitation/emission matrices (EEM) of nonexposed and exposed BSA samples for increasing reaction times, whereas Figure 2d) shows the fluorescence spectra of native BSA and BSA exposed to O_3 in the liquid phase at λ_{ex} = 320 nm. Clearly, the fluorescence intensity at 400–430 nm increased in the reacted compared to the unreacted BSA samples, which we attribute to the formation of dityrosine species. From the combined SDS-PAGE and fluorescence analysis results, we can infer that ozone induced protein oligomerization occurs via the formation of covalent intermolecular dityrosine cross-links, which is consistent with a previous study.[33]

In another set of homogeneous bulk solution experiments, we investigated the reaction kinetics of the formation of BSA dimers and trimers at O_3 concentrations of 50 and 200 ppb. A series of exposure experiments were conducted for both O_3 concentrations with reaction times between 3 (200 ppb O_3) and 6 (50 ppb O_3) minutes and 2 h. The samples were analyzed by SEC-HPLC-DAD as described above (for exemplary chromatograms, see Supporting Information Figure S3) and the results are shown in Figure 3. Signals corresponding to the molecular weight of BSA dimers, trimers, and even higher oligomers have been observed in the exposed samples. For the

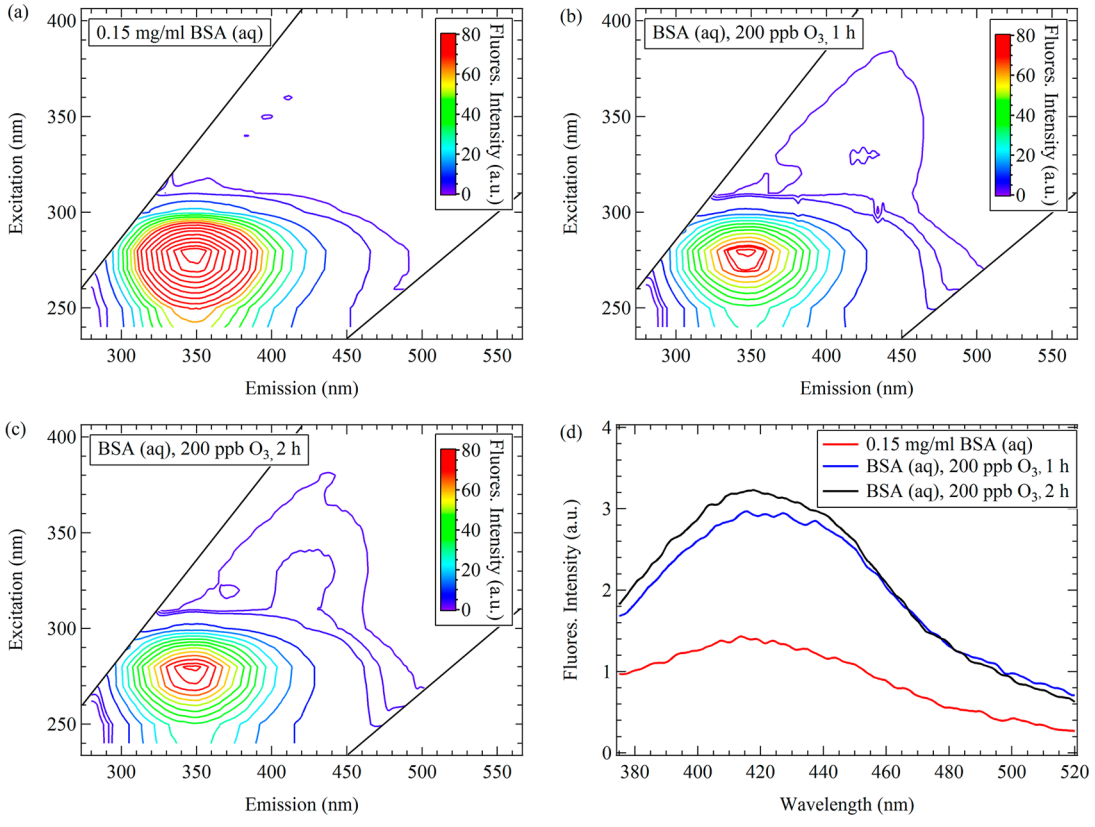

Figure 2. Fluorescence excitation–emission matrices (EEMs) of native BSA (a), and BSA after 1 h (b) and 2 h (c) exposure of 200 ppb O_3 in the liquid phase; (d) fluorescence emission spectra at λ_{ex} = 320 nm (dityrosine signal).

DOI: 10.1021/acs.est.5b02902
Environ. Sci. Technol. 2015, 49, 10859–10866

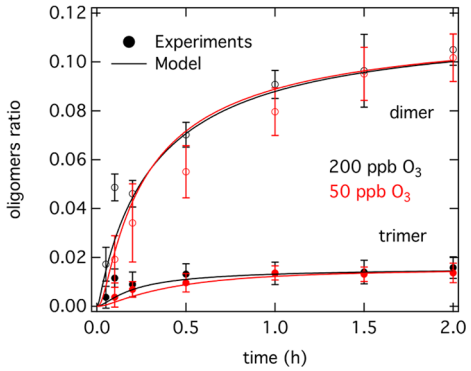

Figure 3. Temporal evolution of protein oligomer content in the aqueous phase reaction of BSA (initial pH 7.1 ± 0.1) with ozone at gas phase concentrations of 50 and 200 ppb O_3. BSA oligomer formation is reported as the temporal evolution of the ratio of the UV signal area (220 nm) of the respective oligomer (dimer, trimer) to the total signal area (sum of monomer and all oligomer signal areas), see section 2.3. The reported values were corrected for the background of dimers and trimers observed in the commercial BSA. The solid lines are results of the kinetic model.

higher oligomers ($MW > MW_{trimer}$), peak shape and retention time varied among different samples. However, according to their retention times, they span a range from tetramers up to decamers.

It should be noted that the ozonolysis of amino acid residues, e.g., Tyr, histidine (His), methionine (Met), and tryptophan (Trp) also results in the formation of oxidized products incorporating O atoms,[34,35] e.g., Tyr + O_3 yields an *o*-quinone derivate.[36] However, in a recent study on the oxidation and nitration of Tyr by O_3 and NO_2, ab initio calculations showed that O_3 can induce H abstraction from the hydroxyl group of the Tyr phenol ring, resulting in the formation of a tyrosyl radical.[37] This reaction was found to have a similar energy barrier as the attack of ozone at the phenol ring in ortho position to the hydroxyl group (3.9 vs 3.6 kcal/mol in aqueous medium).

Oxidative protein cross-links can form upon (a) tyrosyl radical coupling to form dityrosine, (b) Schiff-base cross-linking by reaction of an oxidation-derived protein carbonyl with the ε-amino group of lysine and (c) intra- or intermolecular disulfide cross-linking, in part after reductive separation of pre-existing disulfide bridges.[38] Because we can exclude the formation of intermolecular disulfide bonds as outlined above, the combined SDS-PAGE and fluorescence analysis results, strongly indicate that the observed O_3 induced protein oligomerization can be attributed to the formation of covalent intermolecular dityrosine cross-links.

The formation of tyrosyl radicals during the ozonolysis of BSA may also lead to the formation of O_3^-, which can be rapidly converted into OH radicals. Further, during ozonolysis reactions, $^1O_2$ (singlet oxygen) and H_2O_2 (hydrogen peroxide) are known to occur.[39] These reactive oxygen species (ROS) likely induce secondary reactions, such as oxidation, ring opening of aromatic amino acid side chains, and protein backbone cleavage.[40−42] However, the role of this secondary chemistry in atmospheric protein modification and degradation needs to be investigated in follow-up studies.

The focus of this study was to investigate the chemical process and the kinetics of protein oligomerization under environmentally relevant O_3 and RH conditions. However, the reaction of O_3 with the Tyr residues in BSA likely is site selective. Likely Tyr candidates for this reaction could be inferred from previous work on Tyr nitration in BSA.[20] Protein Tyr nitration by O_3 and NO_2 is a two-step mechanism

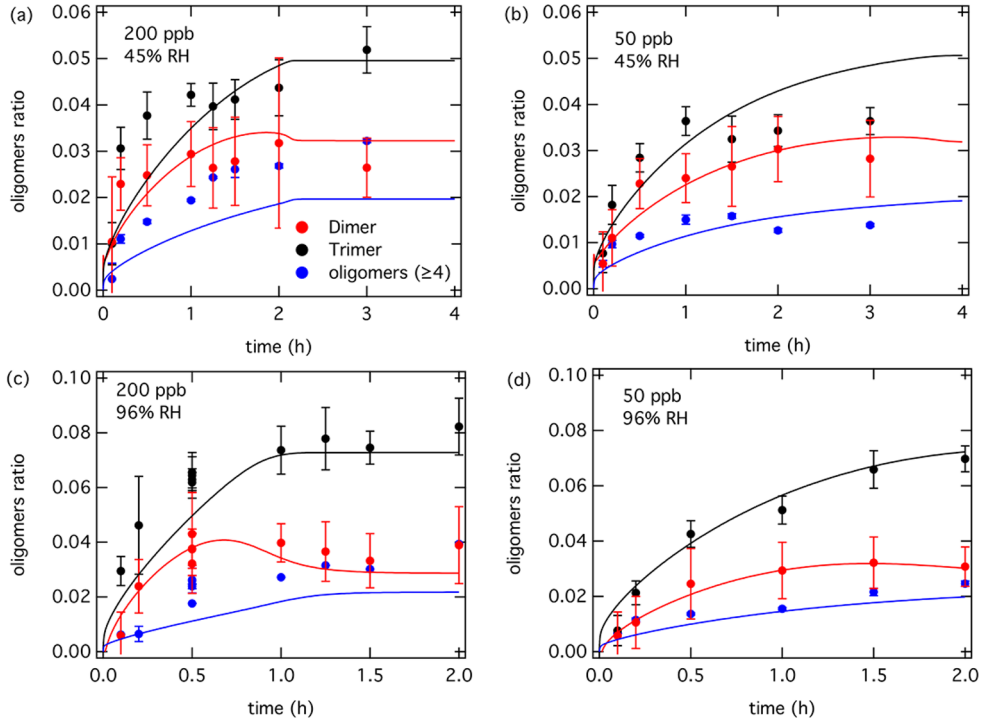

Figure 4. Temporal evolution of protein oligomer content (dimer, red; trimer, black; higher oligomers, blue) upon ozone exposure of BSA films (thickness 34 nm; calculated according to ref 34): (a) 45% RH, 200 ppb O_3; (b) 45% RH, 50 ppb O_3; (c) 96% RH, 200 ppb O3; (d) 96% RH, 50 ppb O_3. Details on experimental conditions and analysis are provided in section 2.3. The solid lines are the results of the kinetic model.

DOI: 10.1021/acs.est.5b02902
Environ. Sci. Technol. 2015, 49, 10859−10866

involving the attack of O_3 as the first step, which is followed by the addition of NO_2 to form 3-nitrotyrosine.[18] Three nitrated Tyr residues (Y161, Y364, and Y520) were found, Y161 was fully nitrated ($ND_{Y161} = 1$), whereas the others exhibited only low nitration degrees ($ND_{Y364} = 0.003$, $ND_{Y520} = 0.006$).[20] However, also other Tyr residues in BSA might be reactive toward O_3, as the nitration involves one more site-selective reaction step than the pure ozonolysis. It should be noted, that for potential dimerization sites, the effect of steric hindrance likely is more important than for the nitration reaction. Further, in a recent study, peroxidase-generated intermolecular dityrosine cross-links in bovine α-lactalbumin were found to be site selective and occurred at sterically favored sites.[43] Tryptophan residues in cytochrome C were observed to be resistant to O_3, whereas Trp in BSA and human serum albumin (HSA) were found to be susceptible to O_3.[44] Such potentially protein structure related resistance may also apply to Tyr in some proteins.

3.2. Kinetics of the Oligomerization Process. Figures 3 and 4 show experimental data and kinetic modeling results to explore and characterize the reaction kinetics of protein oligomerization by ozone. We performed experiments for the reaction of thin protein films (i.e., five layers of protein as detailed below) at 45% RH and 96% RH and proteins in aqueous solution with O_3 gas phase concentrations of 200 and 50 ppb. Oligomer signals were found to increase with exposure time.

Figure 5 illustrates the influence of protein film thickness on the observed increase of oligomer signals after an exposure of

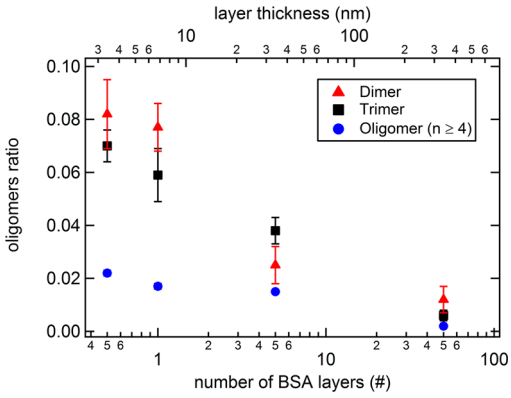

Figure 5. Influence of protein coating thickness on oligomer formation observed after 30 min of ozone exposure (200 ppb O_3, 45% RH).

200 ppb of O_3 for 30 min at 45% RH. For spherical molecules, the number of layers (n) coating the inner surface of the reaction tube can be estimated from their molecular radius (r_m) and the inner diameter (d) and length (l) of the tube: $n = m_{BSA} r_m^2 N_A/(M_{BSA} dl)$, where N_A is the Avogadro constant, 6.022×10^{23} mol^{-1}, $r_m = 3.4$ nm,[45] $M_{BSA} = 66430$ Da. In principle, 2 mg of BSA can form 50 layers on the tube's inner surface. By coating 0.2, 0.04, and 0.02 mg of BSA, five layers, a monolayer, and half of a monolayer can be formed, respectively, assuming an ideal distribution of BSA molecules on the tube's surface. Therefore, when the tube is coated with 0.02 or 0.04 mg of BSA, the reaction with O_3 could be dominated by surface reactions, whereas for 0.2 mg and 2 mg BSA bulk diffusion and reactions plays an increasing role. We found oligomers ratio to be reduced for both the dimer and the trimer with increasing initial BSA mass. Consequently, proteins located on the film surface were oligomerized efficiently, whereas the bulk oligomerization occurred at much slower rates when reactive sites on the surface were consumed, confirming the bulk diffusion limitation result of the kinetic modeling as detailed below.

The observations support that the dimerization of proteins by O_3 proceeds through a chemical mechanism involving two steps, as suggested in previous studies.[18,46] The first step is the reaction of a Tyr residue with O_3 forming phenoxy radical derivatives (tyrosyl radicals) as long-lived reactive oxygen intermediates (ROI-1).[19] It should be noted that O_3 can also oxidize other amino acid residues in proteins such as Trp.[36] However, from other amino acid residues with a high reactivity toward O_3, i.e., cysteine (Cys), Trp, Met, and His,[47] only Cys is able to cross-link proteins directly upon O_3 exposure.[36,48] Cross-linking by O_3 induced intermolecular disulfide bridge formation could be excluded in our experiments (see section 3.1). In the second step of the process, the ROI-1 react with each other to form dimers. A dimer itself can react further with O_3 forming tyrosyl radicals, forming a second type of reactive oxygen intermediate (ROI-2), which may react with ROI-1 to form a trimer. Oxidation of trimer and formation of tetramer is also considered. Further oligomerization was not considered as such products were not detected in significant amount in experimental studies. These reactions can be summarized as follows

$$O_3 + \text{BSA} \rightarrow c_1\text{ROI-1} + (1 - c_1)\ \text{oxidized monomer} \quad \text{(R1)}$$

$$\text{ROI-1} + \text{ROI-1} \rightarrow \text{dimer} \quad \text{(R2)}$$

$$\text{dimer} + O_3 \rightarrow c_2\text{ROI-2} + (1 - c_2)\ \text{oxidized dimer} \quad \text{(R3)}$$

$$\text{ROI-2} + \text{ROI-1} \rightarrow \text{trimer} \quad \text{(R4)}$$

$$\text{trimer} + O_3 \rightarrow c_3\text{ROI-3} + (1 - c_3)\ \text{oxidized trimer} \quad \text{(R5)}$$

$$\text{ROI-2} + \text{ROI-2} \rightarrow \text{tetramer} \quad \text{(R6)}$$

$$\text{ROI-1} + \text{ROI-3} \rightarrow \text{tetramer} \quad \text{(R7)}$$

where c_1, c_2, and c_3 are stoichiometric coefficients for R1, R3, and R5, respectively. The above chemical mechanism was applied in the kinetic model to fit the experimental data. The kinetic parameters were varied using a global optimization method that utilizes a uniformly sampled Monte Carlo search to seed a genetic algorithm (MCGA method[49,50]). The genetic algorithm was terminated when the correlation between experimental data and model output converged into an optimum. Since the optimization of the kinetic parameters to the experimental data was not unique in all kinetic parameters, repeated execution of the MCGA method yields a range of kinetic parameters, which can be used to describe the experimental data (Figure S4). The time and O_3 concentration dependence of dimer and trimer formation in the aqueous phase was reproduced very well, as shown with the solid lines in Figure 3. Concentration of O_3 in the aqueous phase was estimated using a Henry's law constant of 0.011 M atm^{-1}.[51] The second-order rate coefficients for R1 and R3 were found to be fast at $(0.1-5) \times 10^{-14}$ cm^3 s^{-1}, which is consistent with previous studies;[36] the oligomerization rates R2, R4, R6, and R7 were consistently several orders of magnitude lower (see Figure S4). The stoichiometric coefficients c_1 and c_2 were found to be ~0.2, and c_3 was found to be ~0.1.

DOI: 10.1021/acs.est.5b02902
Environ. Sci. Technol. 2015, 49, 10859−10866

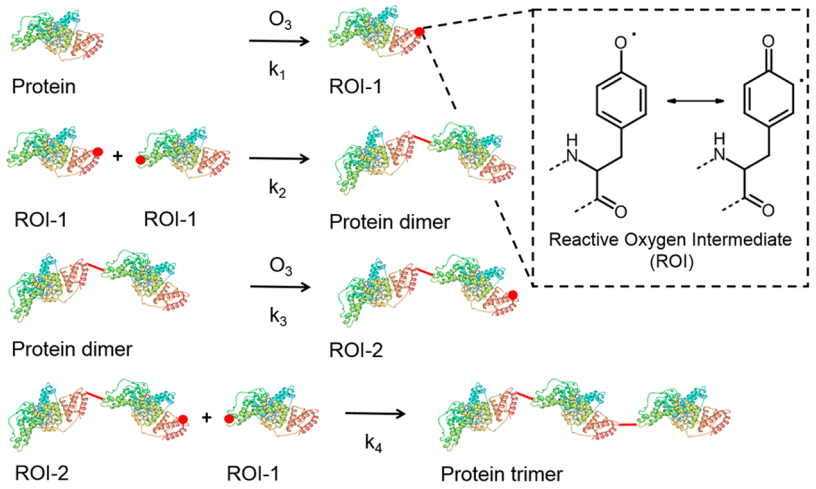

Figure 6. Schematic overview of the most relevant reactions and intermediates for protein oligomerization observed in flowtube experiments upon exposure to environmentally relevant O_3 concentrations. The molecular structure of the protein (bovine serum albumin, BSA; PDB accession number 3V03) was created using the RCSB PDB protein workshop (4.2.0) software.

The reactivity of a Tyr residue is strongly influenced by hydration-level and acidity (pH) of the environment. For instance, phenolate ions are much more reactive toward O_3 than phenols, i.e., by a factor of $\sim 10^6$.[39] However, it is difficult to determine the amounts of conjugated ions of Tyr in our flowtube experiments. Local pH and exact pK_a (of the phenolic hydrogen) values for the individual Tyr residues are hard to determine under these experimental conditions. For aqueous phase experiments, one could calculate the amounts of conjugated Tyr ions according to the Henderson−Hasselbalch equation using the pK_a of the phenolic hydrogen of free Tyr (10.07). According to this equation, $\sim 10^{-5}$ to $\sim 10^{-3}$ dissociated ions per residue should be present at pH 5−7, respectively. By a simple division of the rate constant of Tyr + O_3 calculated by the model in this study ($\sim 6 \times 10^5$−3×10^7 M^{-1} s^{-1}) with the rate constant of phenolate + O_3 reported by Mvula and von Sonntag (1.4×10^9 M^{-1} s^{-1}),[39] we may estimate that $\sim 4 \times 10^{-4}$ to $\sim 2 \times 10^{-2}$ of the reactive Tyr residues in BSA were present in the form of dissociated ions under the experimental conditions applied in this study, indicating neutral to slightly acidic pH in the flow tube experiments. Further, rate constants of Tyr + O_3 reported in the literature (0.7−2.8×10^6 M^{-1} s^{-1} in neutral pH,[52] and 7.2×10^7 M^{-1} s^{-1} in aqueous medium at 298 K calculated using variational transition state theory[37]) are in fairly good agreement with our model results.

Figure 4 shows the temporal evolution of the oligomers ratio (for more details see section 3.1; dimer (red), trimer (black) and oligomers with $n \geq 4$ monomer units (blue)) for O_3 exposure to protein films with gas phase O_3 concentrations of 200 and 50 ppb at 45% and 96% RH. Here, we model the formation of oligomers using the kinetic multilayer model for aerosol surface and bulk chemistry (KM-SUB).[53] KM-SUB explicitly resolves surface-bulk exchange, bulk diffusion and chemical reactions from the gas-particle interface to the particle core, resolving concentration gradients and diffusion throughout the particle bulk. The model fitting to the experimental data for different RH and in aqueous solution was performed using the MCGA method. Optimized parameters include the second-order reaction rate coefficients (see Figure S4), the bulk diffusion coefficients of O_3 in BSA, and the self-diffusion coefficient of the protein.

The solid lines in Figure 4 show the results of model simulations, reproducing the observed evolution of dimer, trimer, and oligomer ($n \geq 4$) concentrations well. The reactive turnover is higher at 96% RH compared to 45% RH, which can be explained by a moisture-induced phase transition of the protein matrix: the phase state of BSA is amorphous solid with high viscosity at 45% RH, whereas it is semisolid or liquid-like with low viscosity at 96% RH.[17] On the basis of the model fitting, the bulk diffusion coefficients of O_3 were estimated to be 10^{-9}−10^{-8} cm^2 s^{-1} at 45% RH and $\sim 10^{-7}$ cm^2 s^{-1} at 96% RH; self-diffusion coefficients of protein were estimated to be $\sim 10^{-17}$ cm^2 s^{-1} at 45% RH and $\sim 10^{-15}$ cm^2 s^{-1} at 96% RH. Protein oxidation followed by oligomerization can be kinetically limited by bulk diffusion particularly at lower RH. In summary, our flow tube experiments show that thin protein films, e.g., on the surface of bioaerosol particles, can be efficiently oligomerized by atmospheric O_3. The most relevant reactions for this process are illustrated in Figure 6.

Temperature also affects the reaction rate of tyrosyl radical formation by ozonolysis. In a recent publication by Sandhiya et al. (2014),[37] the effect of temperature on rate constants of the Tyr + O_3 reactions was studied using ab initio calculations. The rate constant for the formation of tyrosyl radicals in aqueous medium ranged from 3.6×10^6 to 2.7×10^8 M^{-1} s^{-1} over the temperature range of 278−308 K.

Numerous studies indicate that anthropogenic air pollution has led to a massive increase of aerosol and oxidant concentrations in the lower atmosphere. For example, the average mixing ratios of O_3 in continental background air have increased by factors of 2−4 from around 10−20 ppb from the beginning of the 19th century to 30−40 ppb in the 21st century.[54−61] This increase of O_3 concentration in the Anthropocene likely resulted in an increased occurrence of oligomeric proteins in the atmosphere, which in turn may be related to the increase in the prevalence of allergies that has been observed around the globe. The allergenicity of birch pollen has recently been shown to be enhanced at high O_3 concentrations,[62] and the dimeric proteins were found to have higher allergenicity than the monomeric species.[28] On the basis of our observation of higher oligomers formed upon O_3 exposure, we suggest further investigation of the allergenicity of protein oligomers beyond the dimer level.

DOI: 10.1021/acs.est.5b02902
Environ. Sci. Technol. 2015, 49, 10859−10866

In the atmosphere, also, photooxidation of proteins may lead to oligomer formation.[63] Photoinduced radicals can trigger secondary reactions, which have been shown to result in protein cross-linking in the absence of UV radiation.[64] Thus, the reaction mechanism and kinetics presented in this study can be regarded as a lower limit of protein oligomer formation in the atmospheric environment.

■ ASSOCIATED CONTENT

Supporting Information

The Supporting Information is available free of charge on the ACS Publications website at DOI: 10.1021/acs.est.5b02902.

Protein O_3 exposure setup (Figure S1), molecular weight calibration of the size exclusion chromatography (Figure S2), exemplary chromatograms from the SEC-DAD analysis of exposed protein samples (Figure S3) and the second-order reaction rate coefficients determined by applying KM-SUB to experimental data (Figure S4) (PDF).

■ AUTHOR INFORMATION

Corresponding Author

*C. J. Kampf. Phone: +49 (0)6131 39 25877. Fax: +49 (0)6131 39 25336. E-mail: kampfc@uni-mainz.de.

Author Contributions

§These authors contributed equally.

Notes

The authors declare no competing financial interest.

■ ACKNOWLEDGMENTS

F.L. acknowledges financial support from the China Scholarship Council (CSC). T.B. was supported by the Max Planck Graduate Center with the Johannes Gutenberg-Universität Mainz (MPGC), and C.K. acknowledges financial support from the German Research Foundation (DFG Project KA 4008/1-1).

■ REFERENCES

(1) Holgate, S. T. The epidemic of allergy and asthma. *Nature* **1999**, *402* (6760), B2−B4.

(2) Holgate, S. T. The epidemic of asthma and allergy. *J. R. Soc. Med.* **2004**, *97* (3), 103−110.

(3) D'Amato, G.; Baena-Cagnani, C. E.; Cecchi, L.; Annesi-Maesano, I.; Nunes, C.; Ansotegui, I.; D'Amato, M.; Liccardi, G.; Sofia, M.; Canonica, W. G. Climate change, air pollution and extreme events leading to increasing prevalence of allergic respiratory diseases. *Multidscip. Respir. Med.* **2013**, *8*, 12.

(4) Bernstein, J. A.; Alexis, N.; Barnes, C.; Bernstein, I. L.; Nel, A.; Peden, D.; Diaz-Sanchez, D.; Tarlo, S. M.; Williams, P. B.; Bernstein, J. A. Health effects of air pollution. *J. Allergy Clin. Immunol.* **2004**, *114* (5), 1116−1123.

(5) Kampa, M.; Castanas, E. Human health effects of air pollution. *Environ. Pollut.* **2008**, *151* (2), 362−367.

(6) Yang, W.; Omaye, S. T. Air pollutants, oxidative stress and human health. *Mutat. Res., Genet. Toxicol. Environ. Mutagen.* **2009**, *674* (1−2), 45−54.

(7) Connor, A. J.; Laskin, J. D.; Laskin, D. L. Ozone-induced lung injury and sterile inflammation. Role of toll-like receptor 4. *Exp. Mol. Pathol.* **2012**, *92* (2), 229−235.

(8) Ackaert, C.; Kofler, S.; Horejs-Hoeck, J.; Zulehner, N.; Asam, C.; von Grafenstein, S.; Fuchs, J. E.; Briza, P.; Liedl, K. R.; Bohle, B.; Ferreira, F.; Brandstetter, H.; Oostingh, G. J.; Duschl, A. The Impact of Nitration on the Structure and Immunogenicity of the Major Birch Pollen Allergen Bet v 1.0101. *PLoS One* **2014**, *9* (8), e104520.

(9) Gruijthuijsen, Y. K.; Grieshuber, I.; Stocklinger, A.; Tischler, U.; Fehrenbach, T.; Weller, M. G.; Vogel, L.; Vieths, S.; Poschl, U.; Duschl, A. Nitration enhances the allergenic potential of proteins. *Int. Arch. Allergy Immunol.* **2006**, *141* (3), 265−275.

(10) Cuinica, L. G.; Abreu, I.; Esteves da Silva, J. Effect of air pollutant NO2 on Betula pendula, Ostrya carpinifolia and Carpinus betulus pollen fertility and human allergenicity. *Environ. Pollut.* **2014**, *186* (0), 50−55.

(11) Karle, A. C.; Oostingh, G. J.; Mutschlechner, S.; Ferreira, F.; Lackner, P.; Bohle, B.; Fischer, G. F.; Vogt, A. B.; Duschl, A. Nitration of the Pollen Allergen Bet v 1.0101 Enhances the Presentation of Bet v 1-Derived Peptides by HLA-DR on Human Dendritic Cells. *PLoS One* **2012**, *7* (2), e31483.

(12) Hochscheid, R.; Schreiber, N.; Kotte, E.; Weber, P.; Cassel, W.; Yang, H.; Zhang, Y.; Poschl, U.; Muller, B. Nitration of protein without allergenic potential triggers modulation of antioxidant response in Type II pneumocytes. *J. Toxicol. Environ. Health, Part A* **2014**, *77* (12), 679−695.

(13) Motta, A. C.; Marliere, M.; Peltre, G.; Sterenberg, P. A.; Lacroix, G. Traffic-related air pollutants induce the release of allergen-containing cytoplasmic granules from grass pollen. *Int. Arch. Allergy Immunol.* **2006**, *139* (4), 294−298.

(14) Taylor, P. E.; Flagan, R. C.; Miguel, A. G.; Valenta, R.; Glovsky, M. M. Birch pollen rupture and the release of aerosols of respirable allergens. *Clin. Exp. Allergy* **2004**, *34* (10), 1591−1596.

(15) Schappi, G. F.; Taylor, P. E.; Staff, I. A.; Suphioglu, C.; Knox, R. B. Source of Bet v 1 loaded inhalable particles from birch revealed. *Sex. Plant Reprod.* **1997**, *10* (6), 315−323.

(16) Franze, T.; Weller, M. G.; Niessner, R.; Poschl, U. Protein nitration by polluted air. *Environ. Sci. Technol.* **2005**, *39* (6), 1673−1678.

(17) Shiraiwa, M.; Ammann, M.; Koop, T.; Pöschl, U. Gas uptake and chemical aging of semisolid organic aerosol particles. *Proc. Natl. Acad. Sci. U. S. A.* **2011**, *108* (27), 11003−11008.

(18) Shiraiwa, M.; Selzle, K.; Yang, H.; Sosedova, Y.; Ammann, M.; Poschl, U. Multiphase Chemical Kinetics of the Nitration of Aerosolized Protein by Ozone and Nitrogen Dioxide. *Environ. Sci. Technol.* **2012**, *46* (12), 6672−6680.

(19) Shiraiwa, M.; Sosedova, Y.; Rouviere, A.; Yang, H.; Zhang, Y. Y.; Abbatt, J. P. D.; Ammann, M.; Poschl, U. The role of long-lived reactive oxygen intermediates in the reaction of ozone with aerosol particles. *Nat. Chem.* **2011**, *3* (4), 291−295.

(20) Zhang, Y. Y.; Yang, H.; Poschl, U. Analysis of nitrated proteins and tryptic peptides by HPLC-chip-MS/MS: site-specific quantification, nitration degree, and reactivity of tyrosine residues. *Anal. Bioanal. Chem.* **2011**, *399* (1), 459−471.

(21) Selzle, K.; Ackaert, C.; Kampf, C. J.; Kunert, A. T.; Duschl, A.; Oostingh, G. J.; Poschl, U. Determination of nitration degrees for the birch pollen allergen Bet v 1. *Anal. Bioanal. Chem.* **2013**, *405* (27), 8945−8949.

(22) Reinmuth-Selzle, K.; Ackaert, C.; Kampf, C. J.; Samonig, M.; Shiraiwa, M.; Kofler, S.; Yang, H.; Gadermaier, G.; Brandstetter, H.; Huber, C. G.; Duschl, A.; Oostingh, G. J.; Poschl, U. Nitration of the Birch Pollen Allergen Bet v 1.0101: Efficiency and Site-Selectivity of Liquid and Gaseous Nitrating Agents. *J. Proteome Res.* **2014**, *13* (3), 1570−1577.

(23) Verdino, P.; Westritschnig, K.; Valenta, R.; Keller, W. The cross-reactive calcium-binding pollen allergen, Phl p 7, reveals a novel dimer assembly. *EMBO J.* **2002**, *21* (19), 5007−5016.

(24) Lascombe, M. B.; Gregoire, C.; Poncet, P.; Tavares, G. A.; Rosinski-Chupin, I.; Rabillon, J.; Goubran-Botros, H.; Mazie, J. C.; David, B.; Alzari, P. M. Crystal structure of the allergen Equ c 1 - A dimeric lipocalin with restricted IgE-reactive epitopes. *J. Biol. Chem.* **2000**, *275* (28), 21572−21577.

(25) Maleki, S. J.; Kopper, R. A.; Shin, D. S.; Park, C. W.; Compadre, C. M.; Sampson, H.; Burks, A. W.; Bannon, G. A. Structure of the major peanut allergen Ara h 1 may protect IgE-binding epitopes from degradation. *J. Immunol.* **2000**, *164* (11), 5844−5849.

DOI: 10.1021/acs.est.5b02902
Environ. Sci. Technol. 2015, 49, 10859−10866

(26) Niemi, M.; Jylha, S.; Laukkanen, M.-L.; Soderlund, H.; Makinen-Kiljunen, S.; Kallio, J. M.; Hakulinen, N.; Haahtela, T.; Takkinen, K.; Rouvinen, J. Molecular interactions between a recombinant IgE antibody and the beta-lactoglobulin allergen. *Structure* **2007**, *15* (11), 1413−1421.
(27) Niemi, M. H.; Rytkonen-Nissinen, M.; Janis, J.; Virtanen, T.; Rouvinen, J. Structural aspects of dog allergies: The crystal structure of a dog dander allergen Can f 4. *Mol. Immunol.* **2014**, *61* (1), 7−15.
(28) Kofler, S.; Ackaert, C.; Samonig, M.; Asam, C.; Briza, P.; Horejs-Hoeck, J.; Cabrele, C.; Ferreira, F.; Duschl, A.; Huber, C.; Brandstetter, H. Stabilization of the Dimeric Birch Pollen Allergen Bet v 1 Impacts Its Immunological Properties. *J. Biol. Chem.* **2014**, *289* (1), 540−551.
(29) Magler, I.; Nuss, D.; Hauser, M.; Ferreira, F.; Brandstetter, H. Molecular metamorphosis in polcalcin allergens by EF-hand rearrangements and domain swapping. *FEBS J.* **2010**, *277* (12), 2598−2610.
(30) Rouvinen, J.; Janis, J.; Laukkanen, M.-L.; Jylha, S.; Niemi, M.; Paivinen, T.; Makinen-Kiljunen, S.; Haahtela, T.; Soderlund, H.; Takkinen, K. Transient Dimers of Allergens. *PLoS One* **2010**, *5* (2), e9037.
(31) Pöhlker, C.; Huffman, J. A.; Poschl, U. Autofluorescence of atmospheric bioaerosols - fluorescent biomolecules and potential interferences. *Atmos. Meas. Tech.* **2012**, *5* (1), 37−71.
(32) Malencik, D. A.; Sprouse, J. F.; Swanson, C. A.; Anderson, S. R. Dityrosine: Preparation, isolation, and analysis. *Anal. Biochem.* **1996**, *242* (2), 202−213.
(33) Verweij, H.; Christianse, K.; Vansteveninck, J. Ozone-induced formation of O,O'-dityrosine cross-links in proteins. *Biochim. Biophys. Acta, Protein Struct. Mol. Enzymol.* **1982**, *701* (2), 180−184.
(34) Lloyd, J.; Spraggins, J.; Johnston, M.; Laskin, J. Peptide ozonolysis: Product structures and relative reactivities for oxidation of tyrosine and histidine residues. *J. Am. Soc. Mass Spectrom.* **2006**, *17* (9), 1289−1298.
(35) Kotiaho, T.; Eberlin, M. N.; Vainiotalo, P.; Kostiainen, R. Electrospray mass and tandem mass spectrometry identification of ozone oxidation products of amino acids and small peptides. *J. Am. Soc. Mass Spectrom.* **2000**, *11* (6), 526−535.
(36) Sharma, V. K.; Graham, N. J. D. Oxidation of Amino Acids, Peptides and Proteins by Ozone: A Review. *Ozone: Sci. Eng.* **2010**, *32* (2), 81−90.
(37) Sandhiya, L.; Kolandaivel, P.; Senthilkumar, K. Oxidation and Nitration of Tyrosine by Ozone and Nitrogen Dioxide: Reaction Mechanisms and Biological and Atmospheric Implications. *J. Phys. Chem. B* **2014**, *118* (13), 3479−3490.
(38) Stadtman, E. R. Protein oxidation and aging. *Free Radical Res.* **2006**, *40* (12), 1250−1258.
(39) Mvula, E.; von Sonntag, C. Ozonolysis of phenols in aqueous solution. *Org. Biomol. Chem.* **2003**, *1* (10), 1749−1756.
(40) Xu, G.; Chance, M. R. Hydroxyl Radical-Mediated Modification of Proteins as Probes for Structural Proteomics. *Chem. Rev.* **2007**, *107* (8), 3514−3543.
(41) Davies, M. J. Reactive species formed on proteins exposed to singlet oxygen. *Photochem. Photobiol. Sci.* **2004**, *3* (1), 17−25.
(42) Winterbourn, C. C.; Metodiewa, D. Reactivity of biologically important thiol compounds with superoxide and hydrogen peroxide. *Free Radical Biol. Med.* **1999**, *27* (3−4), 322−328.
(43) Heijnis, W. H.; Dekker, H. L.; de Koning, L. J.; Wierenga, P. A.; Westphal, A. H.; de Koster, C. G.; Gruppen, H.; van Berkel, W. J. Identification of the peroxidase-generated intermolecular dityrosine cross-link in bovine α-lactalbumin. *J. Agric. Food Chem.* **2011**, *59* (1), 444−449.
(44) Mudd, J. B.; Dawson, P. J.; Tseng, S.; Liu, F.-P. Reaction of Ozone with Protein Tryptophans: Band III, Serum Albumin, and Cytochrome C. *Arch. Biochem. Biophys.* **1997**, *338* (2), 143−149.
(45) González Flecha, F. L.; Levi, V. Determination of the molecular size of BSA by fluorescence anisotropy. *Biochem. Mol. Biol. Educ.* **2003**, *31* (5), 319−322.
(46) Shiraiwa, M.; Selzle, K.; Poschl, U. Hazardous components and health effects of atmospheric aerosol particles: reactive oxygen species, soot, polycyclic aromatic compounds and allergenic proteins. *Free Radical Res.* **2012**, *46* (8), 927−939.
(47) Pryor, W. A.; Uppu, R. M. A kinetic model for the competitive reactions of ozone with amino acid residues in proteins in reverse micelles. *J. Biol. Chem.* **1993**, *268* (5), 3120−3126.
(48) Cataldo, F. On the action of ozone on proteins. *Polym. Degrad. Stab.* **2003**, *82* (1), 105−114.
(49) Berkemeier, T.; Huisman, A. J.; Ammann, M.; Shiraiwa, M.; Koop, T.; Pöschl, U. Kinetic regimes and limiting cases of gas uptake and heterogeneous reactions in atmospheric aerosols and clouds: a general classification scheme. *Atmos. Chem. Phys.* **2013**, *13* (14), 6663−6686.
(50) Arangio, A. M.; Slade, J. H.; Berkemeier, T.; Pöschl, U.; Knopf, D. A.; Shiraiwa, M. Multiphase Chemical Kinetics of OH Radical Uptake by Molecular Organic Markers of Biomass Burning Aerosols: Humidity and Temperature Dependence, Surface Reaction, and Bulk Diffusion. *J. Phys. Chem. A* **2015**, *119* (19), 4533−4544.
(51) Sander, R. Compilation of Henry's law constants (version 4.0) for water as solvent. *Atmos. Chem. Phys.* **2015**, *15* (8), 4399−4981.
(52) Pryor, W. A.; Giamalva, D. H.; Church, D. F. Kinetics of ozonation. 2. Amino acids and model compounds in water and comparisons to rates in nonpolar solvents. *J. Am. Chem. Soc.* **1984**, *106* (23), 7094−7100.
(53) Shiraiwa, M.; Pfrang, C.; Poschl, U. Kinetic multi-layer model of aerosol surface and bulk chemistry (KM-SUB): the influence of interfacial transport and bulk diffusion on the oxidation of oleic acid by ozone. *Atmos. Chem. Phys.* **2010**, *10* (8), 3673−3691.
(54) Akimoto, H. Global air quality and pollution. *Science* **2003**, *302* (5651), 1716−1719.
(55) Lelieveld, J.; van Aardenne, J.; Fischer, H.; de Reus, M.; Williams, J.; Winkler, P. Increasing ozone over the Atlantic Ocean. *Science* **2004**, *304* (5676), 1483−1487.
(56) Vingarzan, R. A review of surface ozone background levels and trends. *Atmos. Environ.* **2004**, *38* (21), 3431−3442.
(57) Parrish, D. D.; Millet, D. B.; Goldstein, A. H. Increasing ozone in marine boundary layer inflow at the west coasts of North America and Europe. *Atmos. Chem. Phys.* **2009**, *9* (4), 1303−1323.
(58) Tanimoto, H.; Ohara, T.; Uno, I. Asian anthropogenic emissions and decadal trends in springtime tropospheric ozone over Japan: 1998−2007. *Geophys. Res. Lett.* **2009**, *36*, L23802.
(59) Cooper, O. R.; Parrish, D. D.; Stohl, A.; Trainer, M.; Nédélec, P.; Thouret, V.; Cammas, J. P.; Oltmans, S. J.; Johnson, B. J.; Tarasick, D. Increasing springtime ozone mixing ratios in the free troposphere over western North America. *Nature* **2010**, *463* (7279), 344−348.
(60) Fishman, J.; Creilson, J. K.; Parker, P. A.; Ainsworth, E. A.; Vining, G. G.; Szarka, J.; Booker, F. L.; Xu, X. An investigation of widespread ozone damage to the soybean crop in the upper Midwest determined from ground-based and satellite measurements. *Atmos. Environ.* **2010**, *44* (18), 2248−2256.
(61) Pöschl, U.; Shiraiwa, M. Multiphase Chemistry at the Atmosphere−Biosphere Interface Influencing Climate and Public Health in the Anthropocene. *Chem. Rev.* **2015**, *115* (10), 4440−4475.
(62) Beck, I.; Jochner, S.; Gilles, S.; McIntyre, M.; Buters, J. T. M.; Schmidt-Weber, C.; Behrendt, H.; Ring, J.; Menzel, A.; Traidl-Hoffmann, C. High Environmental Ozone Levels Lead to Enhanced Allergenicity of Birch Pollen. *PLoS One* **2013**, *8* (11), e80147.
(63) Pattison, D. I.; Rahmanto, A. S.; Davies, M. J. Photo-oxidation of proteins. *Photochem. Photobiol. Sci.* **2012**, *11* (1), 38−53.
(64) Dubbelman, T. M. A. R.; Haasnoot, C.; van Steveninck, J. Temperature dependence of photodynamic red cell membrane damage. *Biochim. Biophys. Acta, Biomembr.* **1980**, *601* (0), 220−227.

DOI: 10.1021/acs.est.5b02902
Environ. Sci. Technol. 2015, 49, 10859−10866